SUPPLEMENTAL MATERIAL

for

"A unique circulating miRNA profile highlights thrombo-inflammation in Behçet's syndrome"

Authors

Giacomo Emmi[1,2,*]; Giacomo Bagni[1,*]; Elena Lastraioli[1]; Francesca Di Patti[3,4,5]; Alessandra Bettiol[1]; Claudia Fiorillo[6]; Matteo Becatti[6]; Elena Silvestri[2]; Maria Letizia Urban[1,2]; Lorenzo Emmi[7]; Domenico Prisco[1,°] Annarosa Arcangeli[1,4,°]

Affiliations

Department of Experimental and Clinical Medicine, University of Firenze, Firenze, Italy;

[2]SOD Interdisciplinary Internal Medicine-Behçet Center and Lupus Clinic–Azienda Ospedaliero Universitaria Careggi, Firenze, Italy;

[3]Department of Physics, University of Firenze, Sesto Fiorentino, Firenze, Italy;

[4]Center for the Study of Complex Dynamics (CSDC*)***,** Sesto Fiorentino, Firenze, Italy;

[5]Department of Mathematics and Informatics, University of Perugia, Perugia, Italy;

[6] Department of Experimental and Clinical Biomedical Sciences "Mario Serio", University of Firenze, Firenze, Italy;

[7]Department of Neuroscience, Psychology, Drug Research and Child Health, University of Firenze, Firenze, Italy.

[*] G.E. and G.B. share first authorship.

° D.P. and A.A. share senior authorship

Correspence to:

Prof. Annarosa Arcangeli, MD, PhD.

Department of Experimental and Clinical Medicine, University of Firenze,

Viale GB Morgagni 50, 50134, Firenze, Italy.

E-mail annarosa.arcangeli@unifi.it.

SUPPLEMENTAL METHODS

RNA samples concentration and quality control.

Plasma RNA concentration and purity was assessed using the NanoDrop ND-2000 spectrophotometer (Thermo Fisher Scientific Inc., Waltham, Massachusetts, USA). Qualitative sample analysis was performed using the Agilent 2100 Bioanalyzer and Small RNA Assay Chips (5067-1548, Agilent Technologies, Santa Clara, California, USA) to check for any cellular RNA contamination (indicated by 18S and 28S ribosomal RNA peaks presence) and small RNAs peak detection. The presence of cellular RNA species may indeed interfere in plasma microRNAs profiling experiments resulting in a distorted and non-reproducible profile. RNA aliquots were stored at -80°C until use.

Microarray data analysis and candidate miRNAs selection

To compute the number of subjects needed for the microarray screening, we used an online sample size calculator for microarrays (M.D. Anderson Cancer Center; https://biostatistics.mdanderson.org/MicroarraySampleSize/): given 16 subjects for each group and the 470 human miRNAs sequences covered by the array, we were able to achieve 80% power to detect 1.5-fold expression changes and 95% to detect 2-fold changes (by setting desired false discovery rate= 5% and SD= 0.6).

Expression data were extracted from the obtained TIFF images using the Agilent Feature Extraction (AFE) software, version 9.1 (Agilent Technologies, Santa Clara, CA, USA).

Files were then processed using the R library (http://www.r-project.org/) AgiMicroRna package, available on Bioconductor repository (http://www.bioconductor.org).[**47**]

Median background values were subtracted from the median expression values obtained from the AFE software. The quantile method was then applied in order to perform inter-array normalization. Statistical significance of differences between study groups (BS patients *vs* HC) was assessed comparing mean microarray fluorescence intensity values using the Limma differential expression t-test.

Deregulated (DE) miRNAs were identified on the basis of a $p < 0.05$ by two-tailed t-test and $\log_2$-scale fold change > 1 or < -1.

Unsupervised hierarchical clustering analysis was performed within the same AgiMicroRna package.

To account for discrepancies in miRNA nomenclature due to the different miRBase releases, array features names were converted to MIMATIDs (unique mature miRNA accession number) using a mapping file downloaded from miRBase (http://www.mirbase.org).

The microarray dataset generated and analyzed during the current study is available in the NCBI's Gene Expression Omnibus (GEO) database (GEO Series accession number GSE145191).

For the subsequent technical validation, more stringent criteria were applied for candidate miRNAs selection on the basis of higher fold change ($-2 \geq \log_2 FC \geq 2$), *p*-value ($p < 0.05$ by two-tailed t-test) and false discovery rate (FDR < 0.2, calculated using the Benjamini-Hochberg approach) thresholds.

We further narrowed down the analysis to human miRNAs sequences (indicated by the „hsa"prefix) already reported as circulating elements in the miRandola database and for which experimentally validated targets were available in miRTarBase.

Mature miRNAs primers design

For most primer-pairs, the exact mature miRNAs sequences were used as the specific forward primer. However, when they had a too high or low Tm when compared to the universal reverse primer, or if sequences highly overlapped with other mature miRNAs at 3' end region or with any mRNA, primer sequences were modified as described in Yoon et al.[**48**]:

- Adenine residues were added to the 3' end of the primer, or Guanine or Cytosine to the 5', to increase Tm.
- Conversely, bases were removed from the 5' end of the primer in order to decrease Tm.
- All miRNA primers were designed to achieve at least an 18-mer match to the mature target miRNA sequences while being less than 30 bases in length and with a Tm in the 58°C ± 5 range.

All primers and adaptors were purchased as custom DNA oligos from Eurofins Genomics (Eurofins Scientific, Brussels, Belgium) and their sequences are reported in **Supplemental Table 1**.

All primer-pairs specificity was confirmed by both 2% agarose gel amplification products electrophoresis with ethidium bromide staining and melting curve analysis following the respective protocols descried in *Shi et al.*[**29**] in samples included in the technical validation phase (**Supplemental Table 2**).

Real-Time PCR endogenous normalizers selection

One of the main limitations of extracellular circulating miRNAs (ci-miRNAs) analysis in plasma or serum samples is there is still no consensus regarding specific miRNAs to use as endogenous controls when performing relative quantification by PCR**.** Case-specific normalizers have to be therefore identified and tested.

We therefore selected candidate reference miRNAs based on the obtained microarray results. In order to identify only the stable miRNAs between the two groups (BS patients and HC) we applied the following selection criteria: minimal absolute fold change (FC) in the range of 0.8-1.3 between groups, sharing similar properties in patients and controls (p > 0.05), expressed across all samples, unambiguously annotated in miRBase.

Following this approach, we identified hsa-miR-93 (FC= 0.94) and hsa-miR-16 (FC= 1.30) which has already been reported as typically stable in this test environment according to accumulating studies.

A third reference candidate, hsa-miR-191, was also included *a priori* due to its reported role as endogenous normalizer in several studies on plasma samples and commercial PCR assays designed for ci-miRNAs quantification in biofluids.[**49**] Candidate reference miRNAs expression stability between the two experimental groups was assessed via poly(T) adaptor RT-qPCR in our technical validation cohort.

Cq values from each PCR reaction were used for expression levels analysis of all detected reference miRNA candidates.

The gold-standard statistical approaches BestKeeper,[**50**] geNorm,[**51**] NormFinder,[**52**] the comparative ΔCq method [**53**] and the web-based program RefFinder [**54**] were used to determine and rank the stability of the candidate reference miRNAs using software defaults parameters.

While each individual algorithm uses a different statistical approach, RefFinder gives an integrative overall stability ranking based on the geometric mean of the other four over-mentioned methods.

RefFinder analysis gave a comprehensive result ranking hsa-miR-191 as the most stable reference miRNA, followed by hsa-miR-93 and hsa-miR-16 (**Supplemental Fig. 2**). Folds of expression were therefore calculated from triplicate Cq (cycle quantification) values following the $2^{-\Delta\Delta Cq}$ method [**55**] and selecting hsa-miR-191 as normalizer.

Database interrogation

Experimentally validated miRNAs target genes were identified using the online tool miRTarBase (http://miRTarBase.mbc.nctu.edu.tw, release 6.0).[**56**]

In order to investigate if DE miRNAs already had reported roles as circulating elements, we used miRandola database (http://www.mirandola.iit.cnr.it).[**57**]

The online miRWalk version 2.0 tool (http://mirwalk.umm.uni-heidelberg.de) disease ontology-based search was used to identify selected miRNA interactions with genes reported as relevant in BS (disease ontology ID: DOID13241).[**58**]

All the above-mentioned databases interrogations were performed taking into account the top DE human (indicated by the "hsa" prefix) ci-miRNAs selected from the microarray screening analysis (see above).

Functional annotation analysis

Both direct miRNAs to KEEG pathway analysis and Gene Ontology functional annotation were performed using DIANA-miRPath version 3.0 online software based on targets predicted by the DIANA-microT-CDS algorithm (http://www.microrna.gr/miRPathv3).[**30**]

Targets with a microT-CDS score higher than 0.7 were selected. Applying Conservative Stats, enriched terms with $p < 0.05$ and a false discovery rate (FDR) (determined according to the Benjamini-Hoechberg's method) < 0.05, were retained and hence considered as significantly impacted by the DE ci-miRNA profile. Functional annotation analysis was performed taking into account the comprehensive DE human ci-miRNA profile.

REFERENCES

47. López-Romero P. Pre-processing and differential expression analysis of Agilent microRNA arrays using the AgiMicroRna Bioconductor library. *BMC Genomics* 2011;12:64.
48. Yoon H, Belmonte KC, Kasten T, et al. Intra- and Inter-individual Variability of microRNA Levels in Human Cerebrospinal Fluid: Critical Implications for Biomarker Discovery. *Sci Rep* 2017;7:12720.
49. Bertoia ML, Bertrand KA, Sawyer SJ, et al. Reproducibility of Circulating MicroRNAs in Stored Plasma Samples. *PLoS One* 2015;10:e0136665.
50. Pfaffl M.W, Tichopad A, Prgomet C, et al. Determination of stable housekeeping genes, differentially regulated target genes and sample integrity: BestKeeper--Excel-based tool using pair-wise correlations. *Biotechnol Lett* 2004;26;509-515.
51. Vandesompele J, De Preter K, Pattyn F, et al. Accurate normalization of real-time quantitative RT-PCR data by geometric averaging of multiple internal control genes. *Genome Biol* 2002;3:RESEARCH0034.
52. Andersen CL, Jensen JL, Ørntoft TF. Normalization of real-time quantitative reverse transcription-PCR data: a model-based variance estimation approach to identify genes suited for normalization, applied to bladder and colon cancer data sets. *Cancer Res* 2004;64:5245-5520.
53. Silver N, Best S, Jiang J, et al. Selection of housekeeping genes for gene expression studies in human reticulocytes using real-time PCR. *BMC Mol Biol* 2006;7:33.
54. Xie F, Xiao P, Chen D, et al. miRDeepFinder: a miRNA analysis tool for deep sequencing of plant small RNAs. *Plant Mol Biol* 2012;80:75–84.
55. Livak KJ, Schmittgen TD. Analysis of relative gene expression data using real-time quantitative PCR and the 2(-Delta Delta C(T)) Method. *Methods* 2001;25:402-408.

56. Chou CH, Shrestha S, Yang CD, et al. miRTarBase update 2018: a resource for experimentally validated microRNA-target interactions. *Nucleic Acids Res* 2018;46:D296-D302.
57. Russo F, Di Bella S, Nigita G, et al. miRandola: extracellular circulating microRNAs database. *PLoS One* 2012;7:e47786.
58. Dweep H, Sticht C, Pandey P, et al. miRWalk--database: prediction of possible miRNA binding sites by "walking" the genes of three genomes. *J Biomed Inform* 2011;44:839-847 .

Supplemental Table 1

Current miRNA ID	Primer sequence (5' - 3')	Length (NTs)	GC (%)	Tm (C°)
hsa-miR-187	GTCTTGTGTTGCAGCCGGAA	20	55	59.3
hsa-miR-411	TAGTAGACCGTATAGCGTACG	21	47,6	58.0
hsa-miR-27a	TTCACAGTGGCTAAGTTCCGC	21	52,4	59.8
hsa-miR-206	TGGAATGTAAGGAAGTGTGTGG	22	45,5	58.4
hsa-miR-224	CAAGTCACTAGTGGTTCCGTT	21	47,6	58.0
hsa-miR-653	CGTGTTGAAACAATCTCTACTGAA	24	37.5	57.6
hsa-miR-16	TAGCAGCACGTAAATATTGGCG	22	45,4	58.4
hsa-miR-191	GAATCCCAAAAGCAGCTGAAA	21	42,9	58.8
hsa-miR-93	CAAAGTGCTGTTCGTGCAA	19	47.4	58
Universal Reverse primer	GCGAGCACAGAATTAATACGAC	22	45,5	58,4
Poly(T) adaptor	GCGAGCACAGAATTAATACGACTCACTATAGGTTTTTTTTTTTT(12)VN			

Supplemental Table 2

	BS patients	**Healthy controls**
Number of subjects observed	5	5
Sex *(n, %)*		
Male	2	2
Female	3	3
Age *Mean (IQR; range)*	42.8 (3; 42-48)	36.6 (15; 29-54)
HLA-B51 *(n, %)*		
Positive	4 (80)	
Active manifestations at time of sample collection (ICBD criteria) *(n, %)*		
Oral aphtosis	5 (100)	
Skin involvement	4 (80)	
Articular involvement	3 (60)	
Neurologic involvement	3 (60)	
Ocular involvement	2 (40)	
Genital aphtosis	1 (20)	
Vascular involvement	1 (20)	
Intestinal involvement	1 (20)	
Pseudofolliculitis	1 (20)	
Disease activity at time of sample collection *(n, %)*		
Active (BDCAF≥1)	3 (60)	
Non Active (BDCAF=0)	2 (40)	
On treatment at time of sample collection	3 (60)	

Supplemental Table 3

miRNA ID	Target Genes	PMID
hsa-miR-187-3p	**TNF** FOXA2 BCL6	(23071313) (28098868) (26845350)
hsa-miR-411-5p	**MICA** **IL18** GRB2	(23824327) (25231602) (27264952)
hsa-miR-27a-3p	**IFNG**, SEMA7A, TGFBR1 PPARG **FOXO1**	(23071313) (24725595) (32528555) (24244514) (22213032)
hsa-miR-206	**BCL2** KRAS **VEGF** NOTCH3	(24855559) (25246801) (27318091) (19723635)
hsa-miR-224-5p	**BCL2** PTX3 CD40 MTOR	(22989374) (24470395) (19475450) (27315344)
hsa-miR-653-5p	**BCL2** TFPI STAT2 **TRIM9**	(33495824) (23592263) (30623419) (30703767)

Supplemental Table 4

Current ID	miRandola annotation	Location	Source
hsa-miR-411	Potential biomarker for cancer detection (18663219), breast cancer (22353773).	Free-Circulating	Plasma Serum
hsa-miR-187	Potential biomarker for ovarian cancer (18589210).	Free-Circulating Exosomes	Urine Serum
hsa-miR-27a	Potential biomarker for lung cancer (22389695), potential biomarker for type 1 diabetes (22829805), potential glioblastoma biomarker (19011622), papillary adenocarcinoma of ovary (18589210), potential biomarker for cancer detection (18663219), detected in blood microvescicles (19002258), carried by Argonaute2 complex (21383194), transferred from t cells to antigen-presenting cells (21505438), heart failure (22120965).	Free-Circulating	Urine Serum
hsa-miR-206	Papillary adenocarcinoma of ovary (18589210), rhabdomyosarcoma (20696132), potential pertussis biomarker (23073777), amyotrophic lateral sclerosis (24586506), potential biomarker for asthma (27362794).	Free-Circulating Exosomes	Serum
hsa-miR-224	Papillary adenocarcinoma of ovary (18589210), potential biomarker for cancer detection (18663219), hepatocellular carcinoma (20815808), liver cirrosis (20815808), characterization of healthy subjects extracellular miRNome (21609964).	Free-Circulating	Serum
hsa-miR-653	Glioblastoma (25950799), myelodysplastic syndroms (25216221).	Free-Circulating	Plasma

Supplemental Table 5

KEGG terms	p-value	#genes	#miRNAs
ECM-receptor interaction	2.97854778143e-07	19	3
Proteoglycans in cancer	8.15776136552e-06	45	3
Gap junction	1.45220109838e-05	26	3
Glioma	3.12355498282e-05	20	3
Rap1 signaling pathway	8.56865117068e-05	52	3
Estrogen signaling pathway	0.000120415379065	25	3
Thyroid cancer	0.000390366023966	10	3
Prostate cancer	0.000498305945277	26	3
Hippo signaling pathway	0.000514901175224	38	3
Morphine addiction	0.00054282599186	20	3
Glycosphingolipid biosynthesis - lacto and neolacto series	0.000705868355122	7	3
Adrenergic signaling in cardiomyocytes	0.00077710915502	34	3
Melanoma	0.000960213296402	22	3
Signaling pathways regulating pluripotency of stem cells	0.00178042372651	34	3
cAMP signaling pathway	0.00326812348543	47	3
Focal adhesion	0.00350174357831	48	3
Glutamatergic synapse	0.00370824349385	27	3
GABAergic synapse	0.00467584637561	19	3
Mucin type O-Glycan biosynthesis	0.00513500981282	6	3
Renal cell carcinoma	0.00540951211244	21	3
Retrograde endocannabinoid signaling	0.00593231793134	24	3
TGF-beta signaling pathway	0.00629520848546	16	3
Ras signaling pathway	0.00694682901452	47	3
Transcriptional misregulation in cancer	0.00717233360192	39	3
Oocyte meiosis	0.00740701572593	28	3
Endometrial cancer	0.00856990957293	16	3
ErbB signaling pathway	0.00942721345947	22	3
Regulation of actin cytoskeleton	0.00958857229959	45	3
Long-term potentiation	0.0108527942635	19	3
Dorso-ventral axis formation	0.0160491234772	10	3
Bacterial invasion of epithelial cells	0.0161003833684	19	3
Long-term depression	0.0177401807909	16	3
Thyroid hormone signaling pathway	0.0208177057901	25	3
Choline metabolism in cancer	0.024050982703	26	3
Adherens junction	0.0257725381843	21	3
Melanogenesis	0.029588847326	22	3
Progesterone-mediated oocyte maturation	0.0305261799381	22	3
Central carbon metabolism in cancer	0.0306993036882	17	3
Amphetamine addiction	0.0307138328738	16	3
cGMP-PKG signaling pathway	0.0316494442725	35	3
Phosphatidylinositol signaling system	0.0318838223254	20	3
Chronic myeloid leukemia	0.0363821315503	18	3
PI3K-Akt signaling pathway	0.044265916492	65	3

Supplemental Table 6

GO:BP terms	p-value	#genes	#miRNAs
organelle	1.68380295908e-93	1486	3
ion binding	5.07912727416e-52	927	3
cellular nitrogen compound metabolic process	2.734024395e-45	727	3
biosynthetic process	7.29548328093e-33	616	3
cellular protein modification process	5.55035581361e-25	378	3
neurotrophin TRK receptor signaling pathway	3.87159421831e-19	64	3
enzyme binding	4.21337734429e-17	225	3
Fc-epsilon receptor signaling pathway	2.05176751702e-16	45	3
molecular_function	1.45175643746e-14	2263	3
protein complex	1.89165353281e-14	551	3
nucleic acid binding transcription factor activity	2.38989655616e-14	173	3
epidermal growth factor receptor signaling pathway	5.4652031774e-12	53	3
blood coagulation	2.02316665446e-11	84	3
macromolecular complex assembly	6.67176169229e-11	147	3
protein binding transcription factor activity	2.38083507943e-09	87	3
small molecule metabolic process	2.38083507943e-09	313	3
cytoskeletal protein binding	8.4490623716e-09	129	3
membrane organization	5.61627052555e-08	96	3
platelet activation	1.04440325131e-07	43	3
enzyme regulator activity	1.5989593938e-07	133	3
fibroblast growth factor receptor signaling pathway	9.59474408806e-07	42	3
phosphatidylinositol-mediated signaling	2.24015693404e-06	33	3
response to stress	3.90769062913e-06	303	3
Fc-gamma receptor signaling pathway involved in phagocytosis	1.80627328477e-05	18	3
cell death	1.80627328477e-05	134	3
synaptic transmission	2.48465785953e-05	69	3
post-translational protein modification	0.000129403387769	29	3
RNA binding	0.000168344133562	254	3
mitotic cell cycle	0.000227763600508	55	3
platelet degranulation	0.000577566858716	17	3
cellular lipid metabolic process	0.000615385146181	26	3
transcription initiation from RNA polymerase II promoter	0.000849488062419	40	3
cellular protein metabolic process	0.00119841840754	59	3
extracellular matrix disassembly	0.00282894790844	21	3
nucleobase-containing compound catabolic process	0.00581722210701	114	3
innate immune response	0.00822932566586	100	3
activation of phospholipase C activity	0.0103219382327	15	3
microtubule organizing center	0.0169927323815	68	3
cytoskeleton organization	0.023020090613	95	3

Supplemental Figure 1

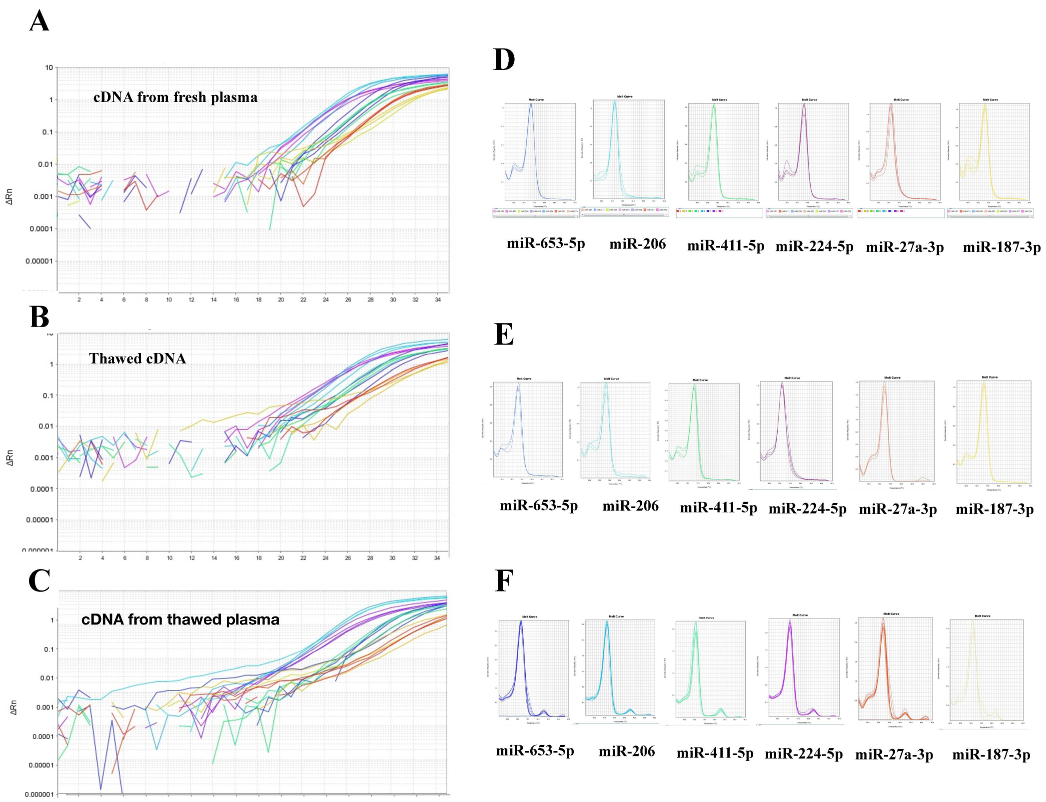

G

	BS	HC
hsa-miR-653-5p	0,09	0,583
hsa-miR-206	0,11	0,0889
hsa-miR-411-5p	0,188	0,143
hsa-miR-224-5p	0,875	0,604
hsa-miR-27a-3p	0,219	0,142
hsa-miR-187-3p	0,293	0,151

Supplemental Figure 2

a

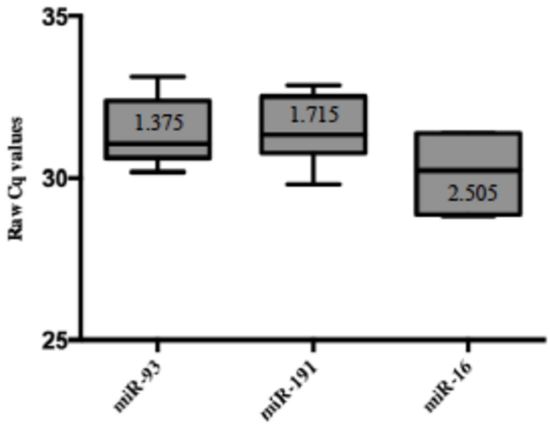

b

	miR-93	miR-191	miR-16
Samples number (*n*)	10	10	10
Cq geomean	31.35	30.39	30.13
Cq arithmetic mean	31.36	30.41	30.15
Minimum Cq (Min)	30.19	30.14	28.84
Maximum Cq (Max)	33.12	32.07	31.40
Standard deviation (SD)	0.98	0.75	1.20
Coefficent of Variation (CV)	3.17	2.50	3.98
Fold Change (FC)	0.992	0.997	0.922
***p*-value (BS*vs* HC)**	0.07	0.07	0.003
Pearson coefficient	0.761	0.842	0.907

c

Method	Ranking Order (Better-Good-Average)		
	1°	**2°**	**3°**
Delta Cq	miR-191 (1.145)	miR-16 (1.214)	miR-93 (1.234)
BestKeeper	miR-93 (0.75)	miR-191 (1)	miR-16 (1.375)
Normfinder	miR-191 (0.681)	miR-16 (0.896)	miR-93 (0.945)
Genorm	miR-191 / miR-16 (1.126)	miR-93 (1.198)	-

d

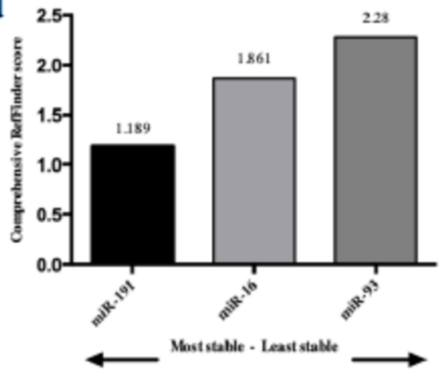

Supplemental Figure 3

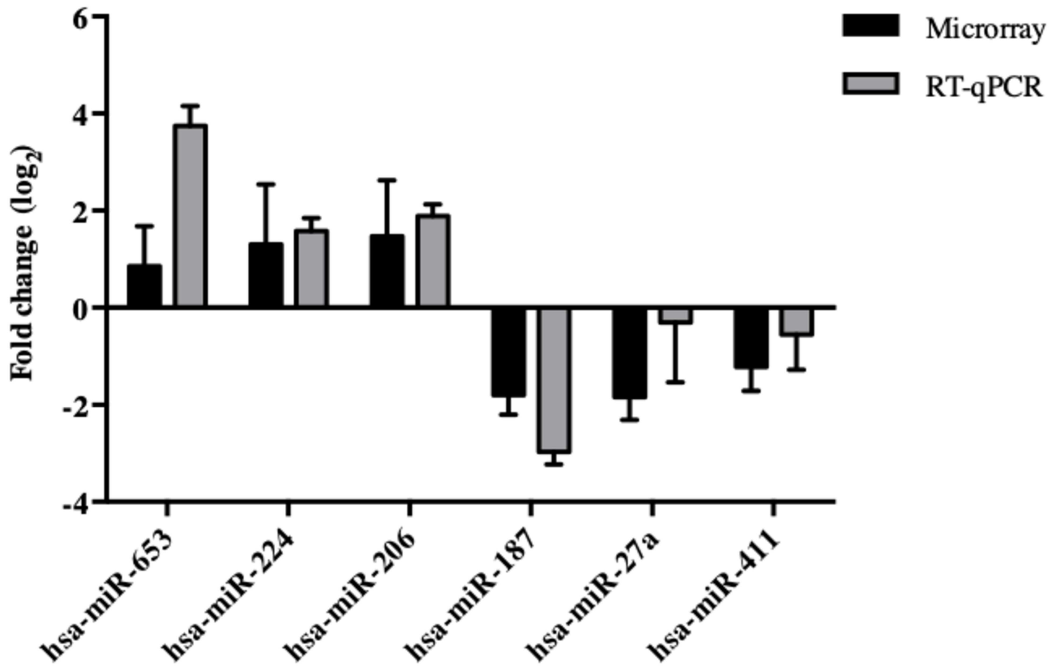

Supplemental Figure 4

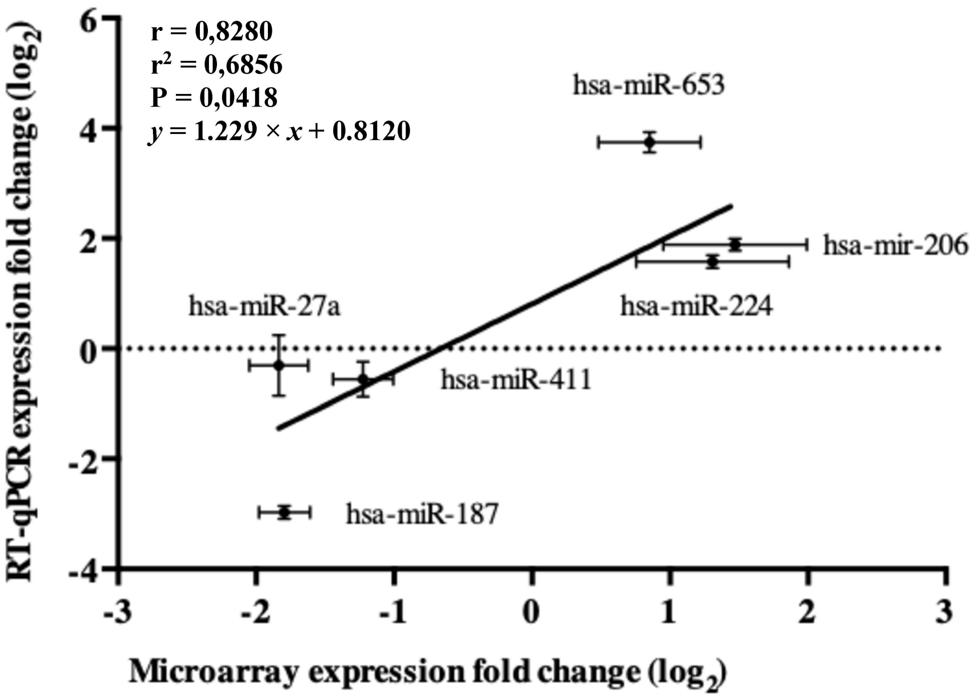

Supplemental Figure 5

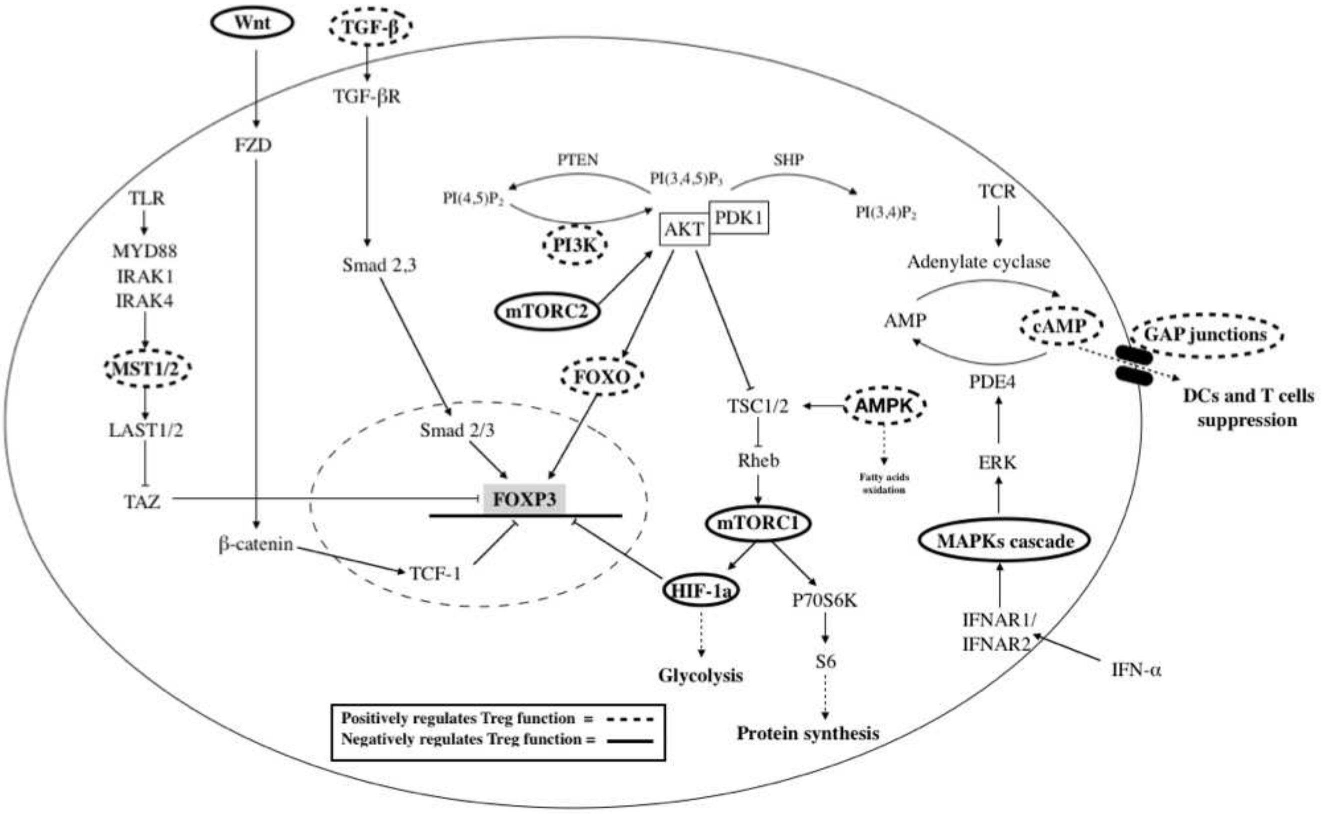

Supplemental Figure 6

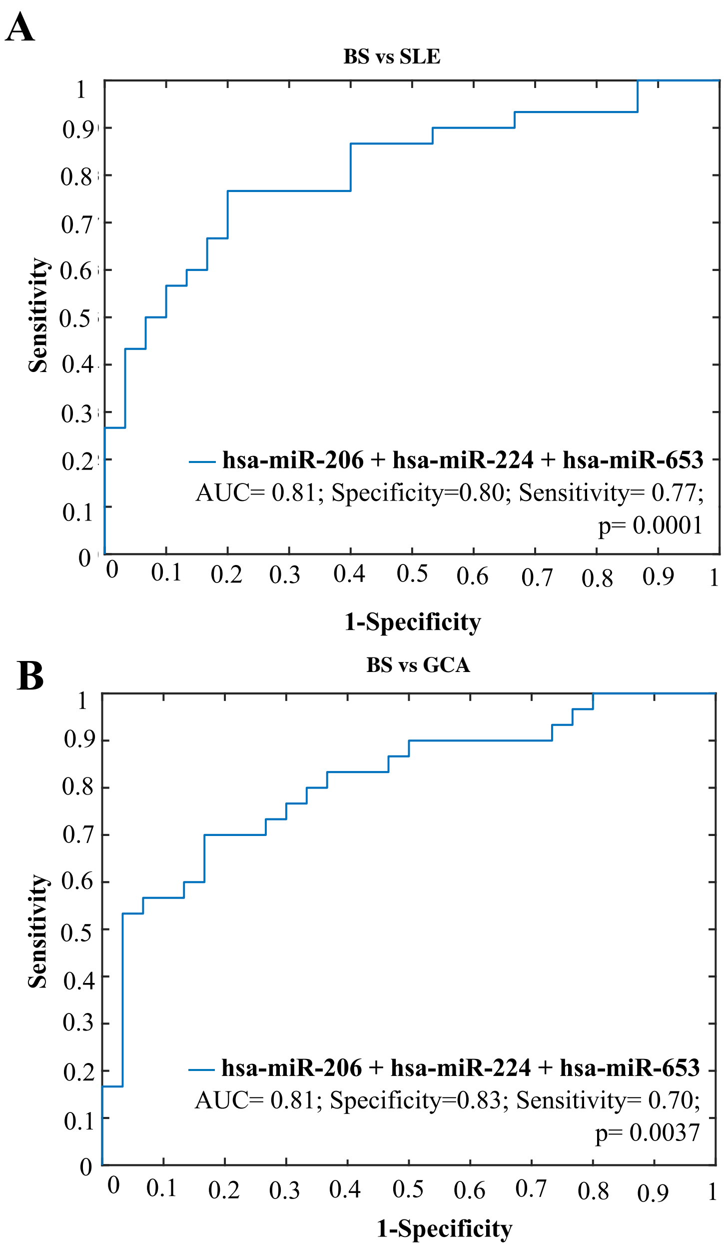

Supplemental Figure 7

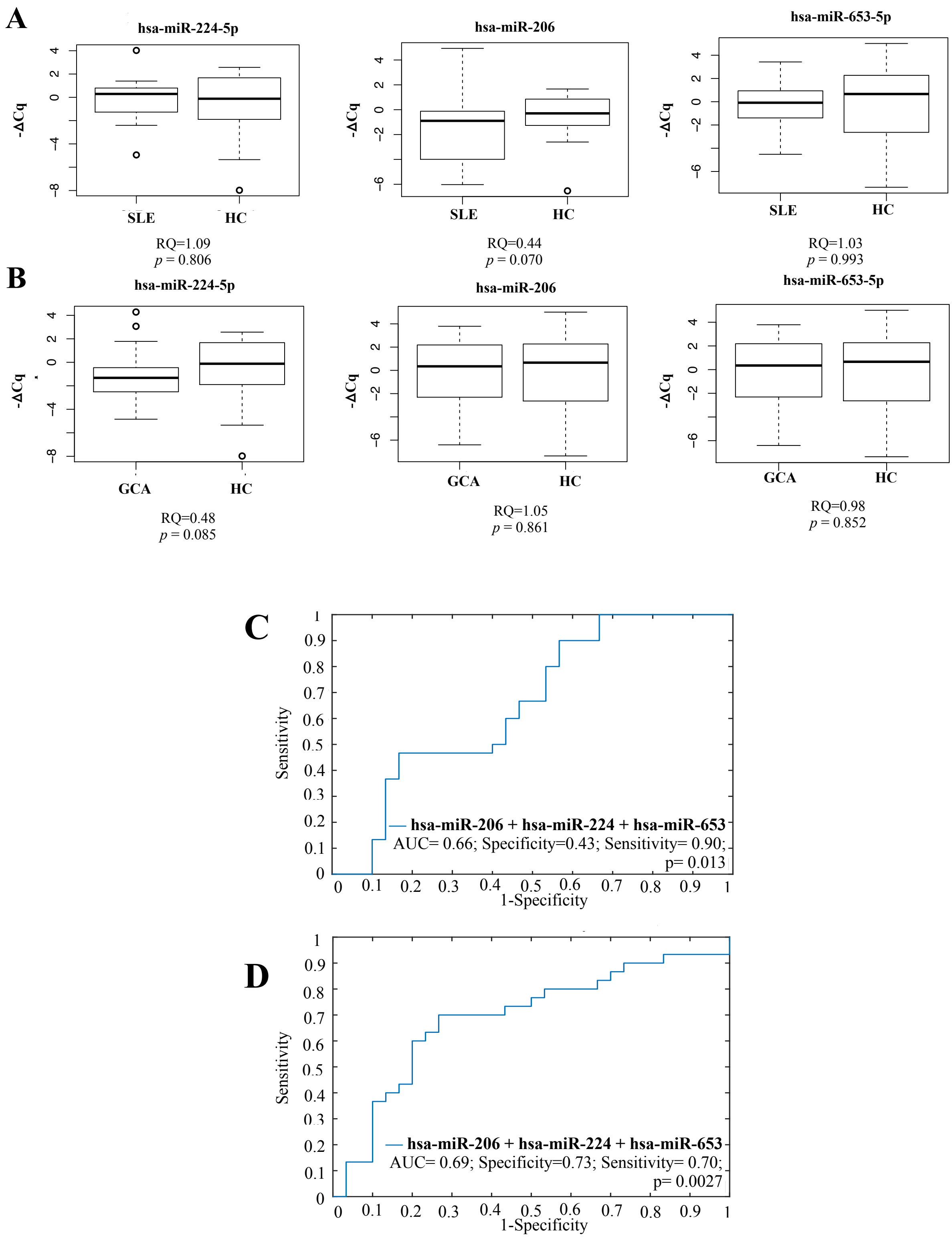

Supplemental Figure 8

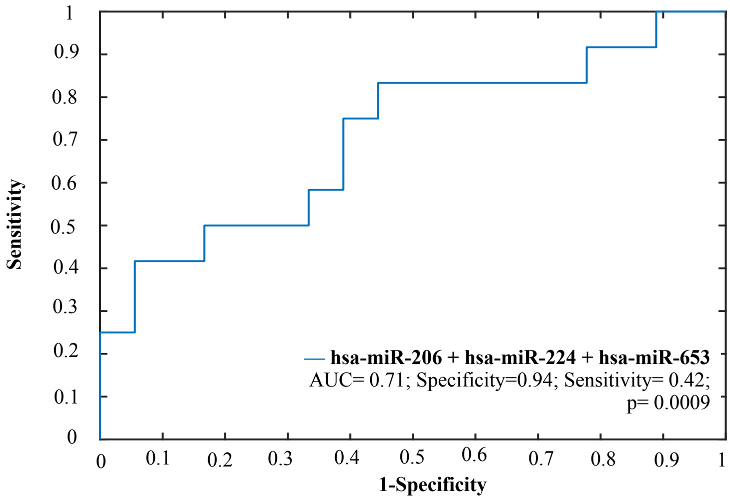

SUPPLEMENTAL FIGURE LEGENDS

Supplemental Table 1: Primers and adaptors sequences used in RT-PCR experiments. Ts=nucleotides; Tm=melting temperature; GC=guanine-cytosine base pairs.

Supplemental Table 2: Technical validation phase subjects' characteristics. CNS= central nervous system. Data are presented as mean ± standard deviation (SD) or n (%) when applicable. IQR=Interquartile Range; BDCAF=Behçet's Disease Activity Form; ICBD=International Criteria for Behçet's Disease. No statistically significant differences were found between groups when analyzing mean age and sex ratio evaluated by Student's T test and Chi-square test respectively.

Supplemental Table 3: Experimentally-validated selected miRNAs targets. Targets in bold are reported susceptibility loci for BS. PMID=PubMed unique IDentifier.

Supplemental Table 4: Selected miRNAs role as circulating elements. Bibliographic references indicating miRNAs potential role as circulating biomarkers are underlined. Bibliographical references are reported in brackets as PMID. miRNAs role as circulating biomarkers in human diseases is reported as underlined annotations. PMID=PubMed unique Identifier.

Supplemental Table 5: Functional Annotation Analysis on the three validated DE miRNAs (KEEG terms). Functional Annotation Analysis was performed on hsa-miR-206, hsa-miR-224-5p and has-miR-653-5p by using DIANA-miRPath v3.0 online tool (genes union mode, FDR-corrected p value threshold=0.05, microT threshold=0.07).

Supplemental Table 6: Functional Annotation Analysis on the three validated DE miRNAs (GO:BP terms). Functional Annotation Analysis was performed on has-miR-206, has-miR-224-5p and has-miR-653-5p by using DIANA-miRPath v3.0 online tool (genes union mode, FDR-corrected p value threshold=0.05, microT threshold=0.07).

Supplemental Figure 1: Comparison between fresh and thawed plasma samples. To assess the replicability of PTA-PCR assays in fresh vs thawed samples, one-way ANOVA was used to compare selected ci-miRNA mean Cq values detected cDNA from fresh plasma, thawed cDNA from fresh plasma and cDNA from thawed plasma derived from a subsets of BS patients and HC from the validation cohort (n=10, 5 BS and 5 HC). All p-values were >0.05.

Representative amplification plots (**A-C**) and melt curves (**D-F**) along with *p*-values from one-way ANOVA (**G**) are reported in the figure. Cq= threshold cycle; BS= Behçet's syndrome patients, HC= healthy controls.

Supplemental Figure 2: Endogenous reference miRNAs selection (RefFinder analysis results). (A) Cq values distribution box whiskers plot of the candidate reference miRNAs across the whole technical validation sample set. The line across the boxes represents the median. Boxes extend from the 25th to the 75th percentile and whiskers show the maximum and minimum values. Interquartile Range (IQR) values are reported in the graph for each candidate reference. (B) BestKeeper statistics results for the three selected candidate reference miRNAs. (C) Reference candidates expression stability ranking order based on different dedicated tools. Stability scores for each algorithm are reported in brackets. (D) Comprehensive stability ranking by RefFinder analysis (a lower geomean value indicates more stable expression). BS= Behçet's syndrome patients; HC=healthy controls. *n*=10 (5 BS and 5 HC).

Supplemental Figure 3: Relative expression fold change (log2) values comparison between microarray and PCR. Data presented as mean ± SEM. *n*=10 (5 BS *vs* 5 HC).

Supplemental Figure 4: Correlation analysis between microarray and RT-qPCR results. r= Pearson correlation coefficient. P=p-value by Two-tailed t-test. *n*=10 (5. BS *vs* 5 HC). Error bars represent standard error of the mean (SEM). *n*=10 (5 BS *vs* 5 HC).

Supplemental Figure 5: Schematic representation of significantly enriched pathways converging on Tregs regulation (comprehensive DE human miRNAs profile KEEG pathway analysis). A complex miRNA-mediated regulation potentially converging on Treg development and function seems to emerge from pathway analysis. DE miRNAs predicted target analysis indeed showed significant enrichment in terms representative of pathways able to either promote or to inhibit Tregs function and development, including AMPK, PI3K-Akt, Foxo, TGF-β, Wnt, mTOR, cAMP, gap junctions, MAPK cascade and HIF signaling.

Supplemental Figure 6: **Selected miRNAs ROC curve analysis (BS vs disease control groups)**. 3 ci-miRNAs combination ROC curve (hsa-miR-206 + hsa- miR-224-5p + hsa-miR-653-5. BS) analysis in BS compared with SLE (**A**) and GCA (**B**). BS= Behçet's syndrome patients; SLE= Systemic lupus erythematosus; GCA= Giant cell arteritis; AUC=Area Under the Curve; *p*= p value (z-test); *n*=60 (30 BS vs 30 SLE or 30 GCA).

Supplemental Figure 7: Selected miRNAs expression in disease control groups compared with healthy controls. (**A, B**) Selected ci-miRNAs PTA-PCR results in LES or GCA compared with HC. Hsa-miR-653-5p (SLE vs HC, RQ=1.03, *p*=0.99; GCA vs HC, RQ=0.98 *p*= 0.85), hsa-miR-224-5p (SLE vs HC, RQ=1.09, *p*= 0.80; GCA vs HC, RQ= 0.48, *p*= 0.08) and hsa-miR-206 (SLE vs HC, RQ= 0.44, *p*= 0.07; GCA vs HC, RQ= 1.05, p= 0.86) showed no significant deregulation in disease control groups when compared to healthy controls. Box and whiskers plots (95% CI). HC= Healthy controls; SLE= Systemic lupus erythematosus; GCA= Giant cell arteritis. Cq = threshold cycle; RQ=relative quantification (ΔΔCq method); *p*=p-value (Mann-Whitney test). *n*=60 (30 SLE or 30 GCA vs 30

HC).(**C, D**) Selected miRNAs ROC curve analysis (disease control groups vs HC). 3 miRNAs combination ROC curve (hsa-miR-206 + hsa- miR-224-5p + hsa-miR-653-5. AUC=Area Under the Curve; *p*= p value (z-test); *n*=60 (30 SLE or 30 GCA vs 30 HC).

Supplemental Figure 8: Selected miRNAs ROC curve analysis (active vs inactive state BS patients). 3 miRNAs combination ROC curve (hsa-miR-206 + hsa- miR-224-5p + hsa-miR-653-5) analysis in active disease state patients compared with inactive disease state ones. Disease activity state is referred to the time of blood sampling.

BS = Behçet's syndrome patients; AUC=Area Under the Curve; *p*= p value (z-test); *n*=30 (12 Active BS patients and 18 inactive disease state BS patients).